IEICE Proceeding Series

Effective Bandwidths of Broadband Chaos

Tsung-Chieh Wu, Yuh-Kwei Chao, Fan-Yi Lin

Vol. 1 pp. 203-206
Publication Date: 2014/03/17
Online ISSN: 2188-5079

2012 International Symposium on Nonlinear Theory and its Applications
NOLTA2012, Palma, Majorca, Spain, October 22-26, 2012

Effective Bandwidths of Broadband Chaos

Tsung-Chieh Wu, Yuh-Kwei Chao, and Fan-Yi Lin†

Institute of Photonics Technologies, Department of Electrical Engineering,
National Tsing Hua University, Hsinchu 30013, Taiwan
† Email: fylin@ee.nthu.edu.tw

Abstract—We propose to use an effective bandwidth in describing the broadband nature of the chaos, which sums up only those discrete spectral segments of the chaos power spectrum accounting for 80% of the total power. Compared to the conventional definitions that tend to overestimate the effective bandwidths of the chaotic signals, the proposed effective bandwidth measures only the bandwidths that possess significant amount of power in the chaos spectra. Using the effective bandwidth proposed, the broadband chaos states can be clearly distinguished from the narrowband periodic oscillation states based on just the values of the effective bandwidths measured without looking into the details of the time series and the spectra. In this study, the bandwidths of the dynamical states generated with an optically injected semiconductor laser under different bandwidth definitions are compared. To demonstrate the usefulness of the proposed definition in applications such as ranging using chaos, the relations between the chaos bandwidths and the peak to sidelobe levels (PSL) are also investigated.

1. Introduction

Chaotic signals have been explored for applications such as fast random-bit generation [1], secured communication [2], and ranging [3]. In these applications, chaos signals with broader spectra are generally preferred which offer the advantages of higher bit-rate and better detection resolution, respectively. While the performances of these applications are directly correlated with the bandwidths of the chaos signals use, an universal definition of the bandwidth for the broadband chaotic signals has not yet been established.

Due to the chaotic and broadband nature of the chaotic signals, the conventional 3 dB bandwidth is not suitable to describe their spectral bandwidths. To the best of our knowledge, an alternative definition of the chaotic signals is first proposed as the frequency span from DC to the frequency where 80% of the total power is contained within in their power spectra [4], which has been adopted in many later works [5]. However, the bandwidths with this definition are usually overestimated which includes those low frequency regions with insufficient power presented. To measure only the spectral regions with significant power, a modified definition measuring only the central portion of the spectrum (near the resonance peak) which contains

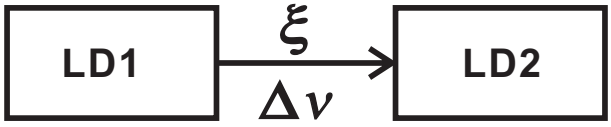

Fig. 1 Schematic setup of an optical injection system. The dynamics of the slave laser (LD2) can be controlled by varying the injection strength ξ and the detuning frequency $\Delta\nu$ from the master laser (LD1).

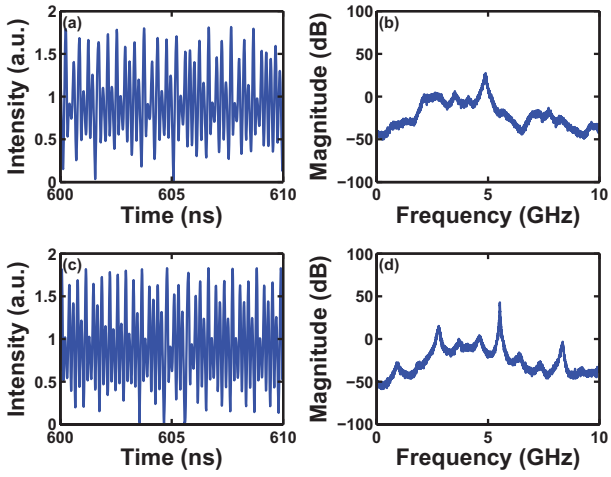

Fig. 2 Time series and power spectra of the chaotic signals generated by an optical injection system under (a)-(b) (ξ, $\Delta\nu$) = (0.05, 2.3) and (c)-(d) (ξ, $\Delta\nu$) = (0.065, 2.3), respectively.

80% of the total power is later proposed and used [6]. Even though the modified definition can better describe the effective bandwidth of the chaotic signals, the fictitious large bandwidths could be mistakenly given for those narrowband periodic oscillation states surrounding the broadband chaos states [7].

Hence, we propose an effective bandwidth for the chaos signals which sums up only those discrete spectral segments of the chaos power spectrum accounting for 80% of the total power. With this definition, the broadband chaos states can be clearly determined based on the values of the effective bandwidths measured. In this study, the bandwidths of different dynamical states generated with an optically injected semiconductor laser under different band-

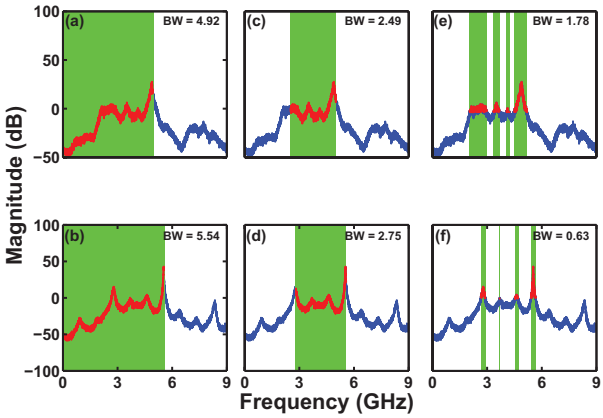

Fig. 3 Bandwidths (BW) (in GHz) of the chaos states shown in Figs. 2(b) and (d) calculated under three different definitions: (a)-(b) the frequency span from DC to the frequency where 80% of the total power is contained within, (c)-(d) the central portion of the frequency span where 80% of the total power is contained within, and (e)-(f) the effective bandwidths which sum up only those discrete spectral segments accounting for 80% of the total power, respectively. The shaded areas denote the spectral spans that have been counted toward the bandwidths given.

width definitions are compared. To demonstrate the usefulness of the proposed definition in applications such as ranging using chaos, the relation between the peak to sidelobe levels (PSL) of the autocorrelations and the bandwidths are also investigated [8].

2. Simulation model

Figure 1 shows the schematic setup of an optical injection laser system. The dynamics of the slave laser (LD2) can be modeled by the following coupled rate equations [3]:

$$\frac{da}{dt} = \frac{1}{2}\left[\frac{\gamma_c\gamma_n}{\gamma_s\tilde{J}}\tilde{n} - \gamma_p(2a+a^2)\right](1+a) + \xi\gamma_c\cos(2\pi\Delta\nu t+\phi) \quad (1)$$

$$\frac{d\phi}{dt} = -\frac{b}{2}\left[\frac{\gamma_c\gamma_n}{\gamma_s\tilde{J}}\tilde{n} - \gamma_p(2a+a^2)\right] - \frac{\xi\gamma_c}{1+a}\sin(2\pi\Delta\nu t+\phi) \quad (2)$$

$$\frac{d\tilde{n}}{dt} = -\gamma_s\tilde{n} - \gamma_n(1+a)^2\tilde{n} - \gamma_s\tilde{J}(2a+a^2) + \frac{\gamma_s\gamma_p}{\gamma_c}\tilde{J}(2a+a^2)(1+a)^2 \quad (3)$$

where a is the normalized optical field, ϕ is the optical phase difference, $\tilde{n}$ is the normalized carrier density, $\tilde{J}$ is the normalized bias current, γ_c is the cavity decay rate, γ_n is the differential carrier relaxation rate, γ_p is the nonlinear carrier relaxation rate, γ_s is the spontaneous carrier relaxation rate, and b is the linewidth enhancement factor. The intrinsic parameters used for the slave laser are $b = 4$, $\gamma_n = 1.334\times10^9 s^{-1}$, $\gamma_p = 2.4\times10^9 s^{-1}$, $\gamma_s = 1.458\times10^9 s^{-1}$, $\gamma_c = 2.4\times10^{11} s^{-1}$, and $\tilde{J} = 0.666$ [6].

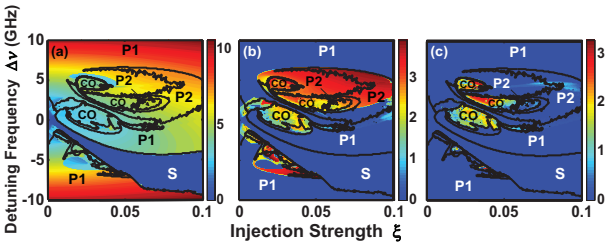

Fig. 4 (a)-(c) Mappings of the bandwidths of different dynamical states in the injection parameter space under the definitions as given in Figs. 3(a)-(b), 3(c)-(d), and 3(e)-(f), respectively. S: stable locking, CO: chaos oscillation, P1: period-one oscillation, and P2: period-two oscillation. The color bars denote the bandwidths of the dynamical states in GHz.

3. Results and Discussions

Figures 2 shows the time series and the power spectra of two typical chaos states obtained with (a)-(b) $(\xi,\Delta\nu) = (0.050, 2.3)$ and (c)-(d) $(\xi,\Delta\nu) = (0.065, 2.3)$ from an optically injected semiconductor laser, respectively. These states will be used as the examples to compared the validity of different bandwidth definitions.

We compare three different definitions of the chaos bandwidths in our investigation, which include (1) the frequency span from DC to the frequency where 80% of the total power is contained within, (2) the central portion of the frequency span where 80% of the total power is contained within, and (3) the proposed effective bandwidth which sums up only those discrete spectral segments accounting for 80% of the total power. Figures 3(a), (c), and (e) and Figs. 3(b), (d), and (f) calculate and compare the bandwidths of the chaos spectra shown in Figs. 2(b) and (d) under these three respective definitions, where the shaded areas in the spectra denote the spectral spans that have been counted toward the bandwidths (BW) given.

As shown in Figs. 3(a) and (b), the bandwidths calculated under the first definition are significantly influenced by the frequency of the resonance peak. In these cases, the effective bandwidths are tend to be overestimated since that the low frequency regions (< 2 GHz) with relatively small magnitudes have been counted toward the chaos bandwidths. To correct the bandwidth with insufficient power at the low frequency region, the second definition measuring only the center portion of the frequency span containing 80% of the total power is also used. However, as can be seen in Fig. 3(d), the bandwidth is mostly determined by

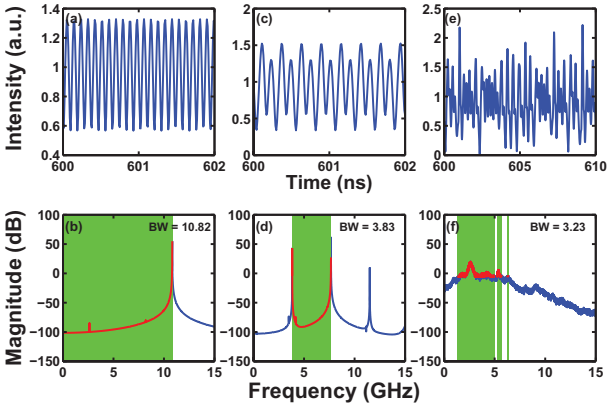

Fig. 5 The time series and the power spectra of the states that have the largest bandwidths under each definition from the mappings shown in Figs. 4(a)-(c). The injection parameters for these states are $(\xi, \Delta\nu) = (0.1, 10)$, (0.083,5.9), and (0.036,4.6), respectively. The shaded areas denote the spectral spans that have been counted toward the bandwidths given.

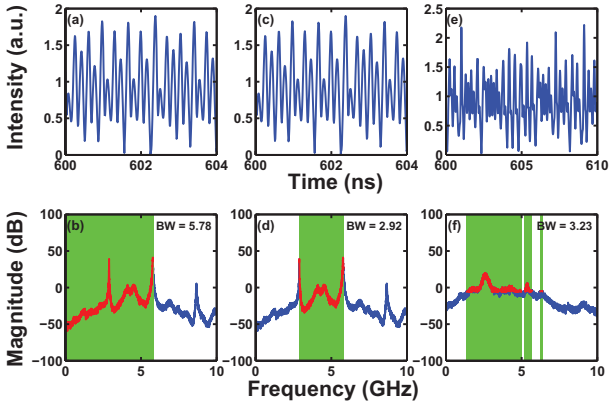

Fig. 6 The time series and the power spectra of the predetermiend chaos states that have the largest bandwidths under each definition from the mappings shown in Figs. 4(a)-(c). The injection parameters for these states are $(\xi, \Delta\nu) = (0.0685, 2.5)$, (0.0685,2.5), and (0.036,4.6), respectively. The shaded areas denote the spectral spans that have been counted toward the bandwidths given.

the frequency difference between the resonance peak and the second highest peak. Inevitably, the magnitudes of the spectral components between and outside these two peaks are not going to substantially affect the chaos bandwidth calculated under this definition.

To take into account only those spectral segments that have sufficient powers, the proposed effective bandwidth which sums up only those discrete segments accounting for 80% of the total power in the power spectrum is instead used and the results are shown in Figs. 3(e) and (f). Under this definition, the bandwidths obtained present precisely the effective bandwidths that can be efficiently used.

Figures 4(a)-(c) show the mappings of the bandwidths for different dynamical states [7, 8] in the injection parameter space under the three respective definitions as given in Figs. 3(a)-(b), 3(c)-(d), and 3(e)-(f). The marked regions of each dynamical states are carefully determined from their time series, power spectra, and phase portraits. Under the first definition, as can be seen in Fig. 4(a), the period-one (P1) oscillation states that have a distinct peak of the oscillation frequency in their power spectra (please see Figs. 5(a)-(b) for the characteristics of a P1 oscillation state) have larger bandwidths compared to the chaos oscillation (CO) states and other dynamical states. While larger injection strength and detuning frequency may seem to lead to a greater bandwidth under this conventional definition (as have been reported previously [4]- [6]), the narrowband periodic states have to be carefully excluded from the real broadband chaos states as mentioned previously to avoid ambiguity.

While the P1 states can be better distinguished from the broadband chaos states under the second definition, as shown in Fig. 4(b), the narrowband period-two (P2) oscillation states that have two distinct peaks corresponding to the oscillation frequency and its subharmonic (please see Figs. 5(c)-(d) for the characteristics of a P2 oscillation state) still mistakenly determined to have the relatively larger bandwidths (reddish regions in Fig. 4(b)). Under these definitions that are commonly used for the chaotic signals, the bandwidths calculated may fail to faithfully represent the effective bandwidths of the dynamical states. As can be seen in Fig. 4(c), the bandwidths for the broadband chaos states are clearly distinguished from the narrowband periodic states, where the periodic states have extremely small bandwidths under this definition (bluish region). Therefore, with the proposed definition, the mapping of the bandwidths faithfully correlates with the dynamical states and can be better used as a guidance when generating chaotic signals for broadband applications. From the mappings shown in Figs. 4(a)-(c), the states with the largest bandwidths under each definition are obtained at $(\xi, \Delta\nu) = (0.1, 10)$, (0.083,5.9), and (0.036,4.6), respectively. The time series and the power spectra of these states are shown in Figs. 5(a)-(b), (c)-(d), and (e)-(f), respectively. As can be seen, while a P1 and a P2 states are mistakenly determined to have the largest bandwidths under the first and the second definitions, only the broadband chaos state shown in Figs. 5(e)-(f) determined with the proposed definition has a chaotic time series and an effective broad spectrum. Results obtained by only choosing the states with the largest bandwidths from the predetermined chaos regions in the mappings of Figs. 4(a)-(c) are also given. The time series and the power spectra of the chaos states obtained are shown in Figs. 6(a)-(b), (c)-(d), and 6(e)-(f) with $(\xi, \Delta\nu) = (0.0685, 2.5)$, (0.0685,2.5), and (0.036,4.6), respectively. Compared with the chaos states selected under the first and the second definitions,

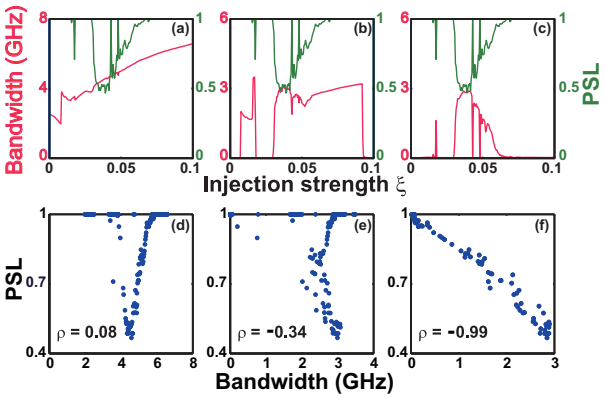

Fig. 7 (a)-(c) The PSLs (green) and the calculated bandwidths (red) using the three respective definitions for those dynamical states obtained in Figs. 4(a)-(c) with $\Delta\nu$ = 2.5 GHz under different injection strengths, respectively. (d)-(f) The replotted PSLs sorted by the respective bandwidths shown in (a)-(c), where ρ are the calculated correlation coefficients.

the chaos state shown in Figs. 6(e)-(f) determined with the proposed definition apparently has a broader effective spectrum.

To further show the usefulness of the effective bandwidth proposed, the PSL of the autocorrelations of the dynamical signals under different injection parameters are calculated. Figures 7(a)-(c) show the PSLs and the calculated bandwidths using the three respective definitions for those dynamical states obtained in Figs. 4(a)-(c) with $\Delta\nu = 2.5$ GHz under different injection strengths, respectively. The PSLs sorted by the respective bandwidths shown in Figs. 7(a)-(c) are replotted in Figs. 7(d)-(f), where their correlation coefficients ρ are also calculated. As can be seen, while no clear correlation between the PSLs and the bandwidths is found under the conventional definitions, the PSL is inversely proportional to the proposed effective bandwidth with a $\rho = -0.99$ as shown in Figs. 7(c) and (f). As the results, from the value of the effective bandwidth, not only the spectral width of a signal but also its periodicity and ambiguity level when used in ranging can be evaluated directly.

4. Conclusions

In conclusion, we have investigated the bandwidths of different dynamical states generated by an optical injection system under three different definitions. The proposed effective bandwidth is shown to better describe the broadband nature of the broadband chaos. From the bandwidths calculated, the broadband chaos states can be clearly distinguished from the narrowband periodic oscillation states without looking into the details of the time series, power spectrum, or phase portrait of each individual state. While the peak oscillation frequency of the chaotic signal is sometime also important and need to be explicitly expressed in applications such as fast random-bit generation and chaotic communications, the usefulness of the effective bandwidth proposed has been demonstrated in applications such as ranging using chaos where the PSLs of the autocorrelations are shown to directly correlate with the effective bandwidths of the chaotic signals.

Acknowledgments

This work is supported by the National Science Council of Taiwan under contract NSC 97-2112-M-007-017-MY3 and NSC 100-2112-M-007-012-MY3 and by the National Tsing Hua University under grant 100N7081E1.

References

[1] K. Hirano, T. Yamazako, S. Morikatsu, H. Okumura, H. Aida, A. Uchida, S. Yoshimori, K. Yoshimura, T. Harayama, and P. Davis, "Fast random bit generation with bandwidth-enhanced chaos in semiconductor lasers,"*J. Opt. Express*, vol.18, pp.5512–5524, 2010.

[2] F. Y. Lin and M. C. Tsai, "Chaotic communication in radio-over-fiber transmission based on optoelectronic feedback semiconductor lasers," *Opt. Express*, vol.10, pp.302-311, 2007.

[3] W. T. Wu, Y. H. Liao, and F. Y. Lin, "Noise suppressions in synchronized chaos lidars," *Opt. Express*, vol.18, pp.26155-26162, 2010.

[4] F. Y. Lin and J. M. Liu, "Nonlinear dynamical characteristics of an optically injected semiconductor laser subject to optoelectronic feedback,"*Opt. Comm.*, vol.221, pp.173–180, 2003.

[5] A. Wang, Y. Wang, and H. He, "Enhancing the bandwidth of the optical chaotic signal generated by a semiconductor laser with optical feedback,"*IEEE Photon. Technol. Lett.*, vol.20, pp.1633–1635, 2008.

[6] F. Y. Lin, S. Y. Tu, C. C. Huang, and S. M. Chang, "Nonlinear dynamics of semiconductor lasers under repetitive optical pulse injection,"*IEEE J. of Sel. Top. Quantum Electron.*, vol.15, pp.604–611, 2009.

[7] S. K. Hwang and J. M. Liu, "Dynamical characteristics of an optically injected semiconductor laser,"*Opt. Comm.*, vol.183, pp.195–205, 2000.

[8] F. Y. Lin and J. M. Liu, "Diverse waveform generation using semiconductor lasers for radar and microwave applications,"*IEEE J. Quantum Electron.*, vol.40, pp.682–689, 2004.